Core-shell hydrogel beads with extracellular matrix for tumor spheroid formation

L. Yu, S. M. Grist, S. S. Nasseri, E. Cheng, Y.-C. E. Hwang, C. Ni, and K. C. Cheung
Electrical and Computer Engineering, University of British Columbia, Vancouver, British Columbia V6T 1Z4, Canada

(Received 23 January 2015; accepted 7 April 2015; published online 17 April 2015)

Creating multicellular tumor spheroids is critical for characterizing anticancer treatments since they may provide a better model of the tumor than conventional monolayer culture. Moreover, tumor cell interaction with the extracellular matrix can determine cell organization and behavior. In this work, a microfluidic system was used to form cell-laden core-shell beads which incorporate elements of the extracellular matrix and support the formation of multicellular spheroids. The bead core (comprising a mixture of alginate, collagen, and reconstituted basement membrane, with gelation by temperature control) and shell (comprising alginate hydrogel, with gelation by ionic crosslinking) were simultaneously formed through flow focusing using a cooled flow path into the microfluidic chip. During droplet gelation, the alginate acts as a fast-gelling shell which aids in preventing droplet coalescence and in maintaining spherical droplet geometry during the slower gelation of the collagen and reconstituted basement membrane components as the beads warm up. After droplet gelation, the encapsulated MCF-7 cells proliferated to form uniform spheroids when the beads contained all three components: alginate, collagen, and reconstituted basement membrane. The dose-dependent response of the MCF-7 cell tumor spheroids to two anticancer drugs, docetaxel and tamoxifen, was compared to conventional monolayer culture. [http://dx.doi.org/10.1063/1.4918754]

I. INTRODUCTION

Cell-based assays are increasingly being used for drug discovery to identify potential drug candidates.[1] Phenotypic, cell-based assays can provide multi-parametric data for quantitative measures of cell response.[2] Although monolayer (i.e., two-dimensional (2-D)) cell culture is widely used, this model lacks cell-cell and cell-extracellular matrix (ECM) signaling, which are essential for functions *in vivo*.[3] Monolayers cannot recreate complex tissue architecture or environmental factors such as oxygen levels which are important for angiogenesis and tumor progression. Thus, three-dimensional (3-D) cell culture will have a strong impact in target validation, secondary screening/lead optimization, and toxicology.[4] Signatures identified from three dimensional cell culture models have been shown to predict clinical outcome in breast cancer data.[5] The microenvironment influences cell behavior and survival by modifying gene expression profile, proliferation, and migration.[6–8] Thus, compared to a monolayer, a multicellular tumor spheroid can better mimic aspects of the tumor *in vivo* including cell-cell contacts,[9] diffusion gradients of oxygen[10] and drugs[11] (when the spheroid is of sufficient size, typically several hundred micrometers in diameter[12–14]), and cell-cell adhesion.[15]

Previous work has found that heterogeneous spheroid sizes can give rise to different levels of hypoxia and thus different gene expression,[16] highlighting the need for good uniformity in spheroid size[17] within an assay. Recent methods to rapidly generate large numbers of uniform spheroids include microfabrication to control numbers of cells sedimenting into wells and thus the resultant spheroid size,[4] robotic dispensing of cells into molded hydrogel templates,[18] and

hanging drop arrays.[19,20] These automated methods improved on previous manual hanging drop, spinning flask, and non-adherent substrate methods which could result in large coefficient of variation (CV) for spheroid size.[12,17,21] These previous spheroids contained cells without ECM components. However, the breast tumor environment contains collagen and other extracellular proteins,[22] which can affect cell architecture[23] and behavior, including phenotype and apoptosis.[24] Basement membrane matrix proteins are an important component of the tumor microenvironment and are produced by carcinoma cells.[25] Ivascu and Kubbies[15] found that the addition of reconstituted basement membrane (Matrigel®) permitted cells to form spheroids with diffusion barriers and quiescent cells, whereas they remained as aggregates with loose cell-cell contacts without Matrigel®. Matrigel® is a reconstituted basement membrane preparation[26] consisting of laminin, collagen IV, and entactin. In addition, type I collagen is a major constituent of the ECM. The normal mammary epithelium and the microenvironment around non-invasive breast tumors includes a dense collagen matrix.[27] Krause *et al.*[26] compared the phenotypes of MCF-7 cells grown in either collagen or in a mixture of collagen and Matrigel® and found that the addition of Matrigel® to the collagen affected the survival and polarization of the MCF-7 cells. The collagen matrix around a tumor micro-environment plays a role in tumor invasion[22,28] and cancer progress.[29] Incorporation of both collagen I as well as reconstituted basement membrane matrix into a three-dimensional culture thus promises to provide an improved tumor spheroid model.

Microfluidic generation of cell-laden hydrogel beads has been demonstrated as a rapid fabrication method for multicellular three-dimensional tissue constructs.[30–34] In this work, we present a microfluidic method to rapidly generate cell-laden hydrogel beads which incorporate elements of the ECM including both collagen I and reconstituted basement membrane matrix proteins. The core-shell structure of the beads was produced in one flow focusing step and used temperature control to maintain both the collagen and reconstituted basement membrane matrix proteins at low temperature below their gel points. The alginate component served as a faster gelling shell which permitted rapid formation of round beads. The encapsulated cells can proliferate to form multicellular spheroids, with applications in drug screening.

II. EXPERIMENTAL METHODS

Reagents were purchased from Sigma-Aldrich Canada Co. (Oakville, Canada) unless otherwise noted.

A. Microfabrication

The microfluidic channels were fabricated using soft lithography.[35] High aspect ratio features were first patterned using SU-8 3050 (MicroChem Corporation, USA) photoresist on a silicon substrate. These features later defined the microchannels and inlet/outlet reservoirs. The SU-8 and silicon structure served as the mold master, onto which poly-(dimethylsiloxane) (PDMS) (Sylgard 184, Dow Corning, USA) was poured. PDMS was cured at 60 °C for 2 h, then the PDMS structure was peeled off the mold master. The droplet formation PDMS structure was then bonded onto a PDMS substrate, forming closed channels. Strong bonding was achieved by first briefly treating the PDMS in plasma; the bonded structures were baked at 65 °C in an oven overnight to recover PDMS hydrophobicity. Access to the inlets and outlets were punched through the elastomer, and fluidic interconnect was made using blunt 21G syringe needle tips (Nordson EFD, USA). The schematic illustration of the core-shell bead formation chip is shown in Fig. 1. The inlet to the junction was 400 μm wide, the junction was 200 μm wide, and the outlets were 1 mm wide. The channel height was 300 μm.

B. Preparation of tumor cell suspensions

MCF-7 breast tumor cells were cultured in RPMI media supplemented with 10% Fetal Bovine Serum (FBS) and 1% penicillin/streptomycin, at 37 °C and 5% CO_2. After washing twice with phosphate buffered saline (PBS), the cells were detached with 0.025 mM trypsin + EDTA

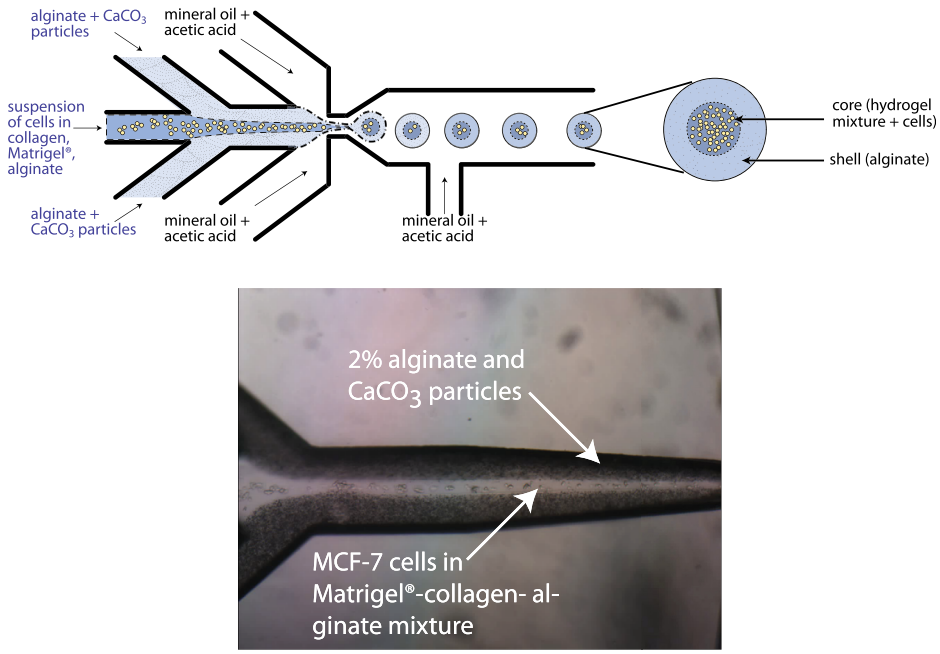

FIG. 1. Flow focusing using two dispersed phases and one immiscible continuous phase forms core-shell beads. Beads are pinched off at the intersection with mineral oil that has been acidified with acetic acid. As the acid diffuses into the beads, it causes the breakdown of the calcium carbonate particles. The released calcium ions then crosslink the alginate, causing the beads to gel. This bead formation method, in which the crosslinking ions are mixed with alginate in an insoluble form and then chemically released, is called internal gelation. This method produces a core-shell structure in which the shell is composed of alginate, and the core is composed of Matrigel® + collagen + alginate in which cells are encapsulated.

and then re-suspended in 1 ml of RPMI media, to which was added 500 μl of 7% bovine serum albumin (BSA) fraction VIII. Cells were then centrifuged, washed in Hank's Buffered Salt Solution (HBSS), centrifuged again, and then resuspended in a solution of PBS.

During preparation of the solution for the bead cores, the collagen and Matrigel® were kept on a small box of ice. Using cooled pipette tips, 100 μl of collagen I at a concentration of 9.21 mg/ml was transferred into cooled conical tubes. Subsequently, 200 μl of Matrigel® (Corning® Matrigel®, VWR International, Mississauga, Ontario, Canada) was added and mixed with the collagen. The mixture was neutralized with approximately 5 μl $NaHCO_3$ to reach pH 7.3–7.5. 50 μl of MCF-7 cells in PBS were added, and the solution was triturated to ensure even dispersion of the cells. Finally, 250 μl of 2% Manucol LKX alginate (FMC Biopolymer, Norway) was added, and the whole solution was tapped vigorously to give a homogeneous mixture with a final cell concentration of approximately 1×10^7 cells/ml. The final concentration of collagen was approximately 1.4 mg/ml. Cell viability prior to mixing into the hydrogel suspension was assessed using Trypan Blue dye exclusion[36] and manual cell counting.

The alginate mixture for the bead shell comprised 2% Manucol LKX alginate with 80 mM $CaCO_3$ mixed with vortexing to ensure even distribution of the $CaCO_3$. The Manucol LKX alginate powder was dissolved in sterile PBS and stirred overnight. $CaCO_3$ particles (J. T. Baker@1301-01) were suspended and sonicated in sterile PBS at the concentration of 2 M. The final concentration of $CaCO_3$ in alginate solution was 80 mM.

C. Core-shell bead generation

Core-shell droplets were generated on the microfluidic chips through flow focusing.[37] Formation of the alginate shell relies on the method of internal gelation.[38,39] Alginate can be gelled in the presence of calcium ions. Calcium, bound in the insoluble form of $CaCO_3$, is mixed into an ungelled alginate solution of high or neutral pH. When the pH is lowered, the acid reacts with the calcium carbonate to release water, CO_2 and Ca^{2+}, initiating alginate

gelation. Here, the oil phase is acidified, and as the alginate droplets spend more time in the oil, more acid will diffuse into the alginate, causing Ca^{2+} release and alginate gelation. Once gelled, the beads can be collected in a tube of culture media, which can be centrifuged to bring the beads down into the aqueous phase.

The oil phase was prepared by mixing 35 ml mineral oil with 0.35 g Span80 (sorbitane mono-oleate nonionic surfactant) and 35 μl acetic acid. The Span80 was used to stabilize the hydrogel droplets and prevent their coalescence prior to gelation.

The core-shell structure was formed on the microfluidic chip using multiple inlet flows in a flow focusing geometry as shown in Fig. 2. The first dispersed phase (1) consisted of collagen, alginate, and Matrigel® mixed with individual cells dispersed in solution, which was chilled in an ice-bath. A concentric tube with continuously flowing ice-cold water was used to chill the collagen + Matrigel® + alginate + cell suspension to prevent gelation prior to droplet formation on chip. The second dispersed phase (2) consisted of alginate precursor and insoluble calcium carbonate particles. The oil served as the immiscible continuous phase (3). Additional acidified mineral oil (4) was added after droplet formation to complete the alginate gelation. The reservoir containing the first dispersed phase (1) was chilled. The flow path between the reservoir and the microfluidic chip was also chilled using a concentric tubing heat exchanger containing ice water in the outer tube annulus and dispersed phase (1) in the inner tube. The outlet of chip (5) flows to the collection vial filled with media, where gel beads were collected.

A pressure-based flow controller (Fluigent, USA) was used to drive the flows in the flow-focusing system. Pressures were adjusted as necessary to obtain droplet bead production. The solutions were introduced into the chip in this order: set the pressure of first and fourth channels at approximately 100 mbar. Once the oil filled the whole chip, pressure in the second and third channels were increased to approximately 75 to 100 mbar. After droplet formation and gelation into beads, beads remained in the chip and tubing for approximately 30 s until they reached the collection tube. At 30-min intervals, the contents of the collection tube (containing oil, beads and media) were centrifuged to isolate the beads, as cells may be damaged from prolonged exposure to the acetic acid.

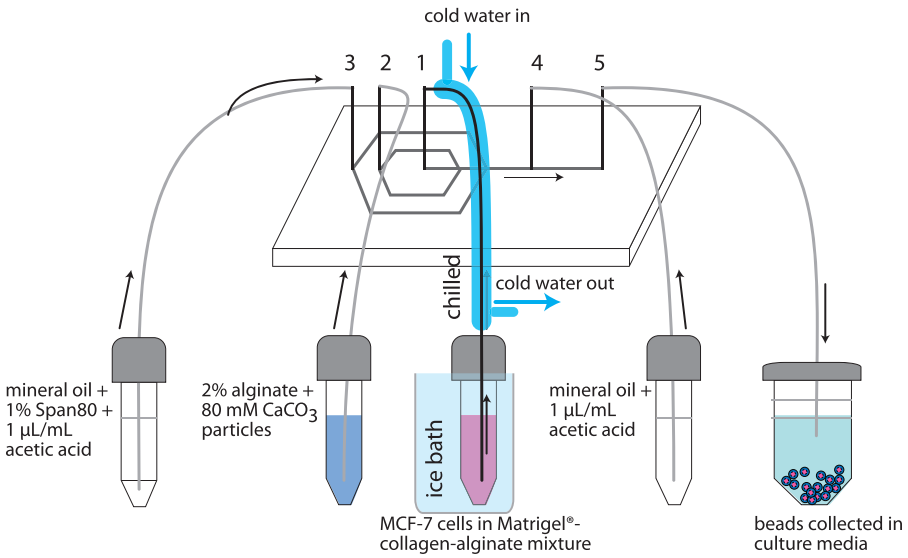

FIG. 2. Schematic of microfluidic chip. Inlets to the chip (1, 2, 3, and 4) are supplied by reservoirs with pressure flow control. The first dispersed phase (1) consisted of Matrigel®, collagen and alginate, with individual cells dispersed in solution. The second dispersed phase (2) consisted of alginate precursor and insoluble calcium carbonate particles. The immiscible continuous phase (3) was mineral oil containing acetic acid. Additional acidified mineral oil (4) was added after droplet formation to increase spacing between the beads and to complete bead gelation. The chip outlet (5) flowed to the collection vial, where gel beads were collected. A concentric tube heat exchanger was used to chill the collagen + Matrigel® + alginate + cell suspension to prevent gelation of the solution prior to droplet formation on chip. Ice-cold water continuously flowed through the annulus while the collagen solution was pumped into the chip.

After collection in the outlet vial (5), the gelled droplets were centrifuged and re-suspended in culture media. Cell viability in the beads was assessed using Trypan Blue dye exclusion and manual cell counting immediately after bead generation. The beads were placed into standard flat bottom, cell culture-treated treated polystyrene culture well plates (Corning), and the well plates were placed into an incubator (5% CO_2, 37 °C).

Bead size was determined by measuring the bead diameter in bright field images using NIS Elements (Nikon Instruments).

D. Assessment of cell proliferation

Cell proliferation was determined using a standard MTS assay (Sigma Aldrich) in which the cell-laden beads were cultured in a 96-well plate. In this type of colorimetric proliferation assay, the quantity of formazan product measured at 450 nm absorbance indicates the number of viable cells in the sample; such proliferation assays can be used with cells embedded within 3-D matrices[40] or with multicellular spheroids.[41] The beads were seeded into standard 96-well plates during the proliferation assay. Cell viability in the beads one day after bead generation was assessed using Trypan Blue dye exclusion and manual cell counting.

E. Second harmonic generation imaging

Second harmonic generation (SHG)[42] imaging was used to visualize the collagen I distribution inside the cell-laden beads. The imaging was performed using an Olympus FV1000MPE with a XLPN25XWMP 25×, 1.05 NA water immersion objective lens. The beads were imaged in custom chambers formed from vinyl adhesive on a glass slide, covered with a #1.5 glass coverslip (0.175 mm thickness). The SHG signal was excited at 810 nm and acquired with a 405 ± 30 nm emission filter removing any back-propagated signal not originating from the collagen fibers.

F. Drug screening

After the cell-laden core-shell beads were generated, they were incubated for 8 days at 37 °C and 5% CO_2 in standard culture flasks. Tamoxifen is a nonsteroidal antiestrogen used to treat breast cancer[43] and tamoxifen treatment will induce cell cycle arrest.[44] Docetaxel has been used to treat breast, prostate, and non-small cell lung cancer, and causes cell death by binding to microtubules.[45] Tamoxifen and docetaxel from clinical formulations were first diluted in PBS and then culture medium to give the final concentrations of drug with no variation in medium concentrations between samples. Approximately 75 beads were placed in each well of a standard 96-well plate, and each experiment had three replicates. Cells were treated for 72 hours. Cell viability in response to treatment was measured using the MTS assay. Data corresponding to the doses from 0.1 to 1000 μM were fitted to a sigmoidal function using a nonlinear regression (MATLAB, MathWorks) in order to determine the concentration producing 50% growth inhibition (IC_{50}).

III. RESULTS AND DISCUSSION

A. Flow focusing produces core-shell beads with good uniformity

Microfluidic flow focusing produces core-shell beads with good size uniformity. The hydrogel core-shell beads exhibited a narrow size distribution with CV of 0.04 (Fig. 3). The cells proliferate within the Matrigel® and collagen mixture in the core of the beads. Cell viability in the hydrogel suspension prior to bead generation was 95 ± 2% (431 cells counted); cell viability immediately after encapsulation into the beads was 85 ± 3% (618 cells counted); cell viability within the beads one day after bead generation was 93 ± 1.6% (502 cells counted).

The core-shell bead structure assists in maintaining spherical droplet and bead shape. Although alginate gels quickly, other biomaterials such as collagen can offer cues that better mimic the natural extracellular matrix.[3] However, biomaterials such as collagen do not gel as

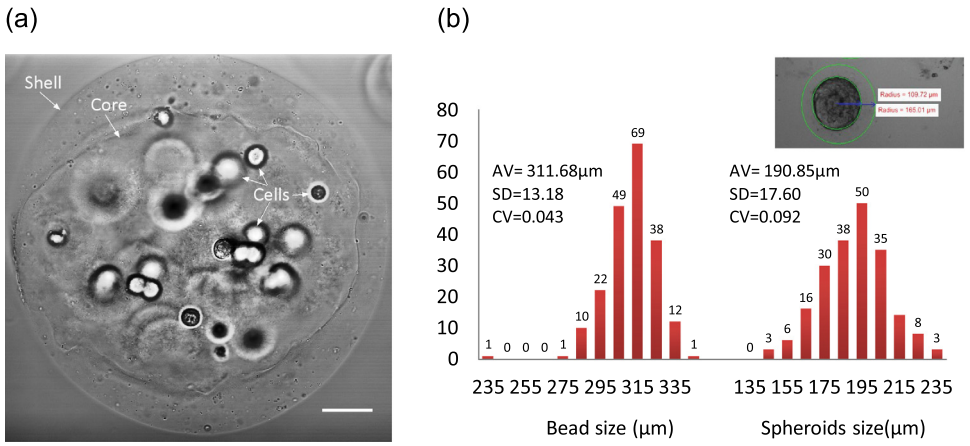

FIG. 3. (a) A transmitted light differential interference contrast image generated by collecting forward-propagating 810 nm excitation light after passing through the sample during a second harmonic generation imaging scan. The core-shell structure is visible after bead collection. Cells are dispersed within the core of the bead. Scale bar represents 50 μm. (b) Size distribution of beads and tumor spheroids. Bead size and spheroid size were measured after 8 days culture.

rapidly as alginate.[46] By using alginate as a fast-gelling component which cross-links quickly in the presence of calcium ions, this microfluidic flow-focusing method creates a core-shell scaffold, wherein the alginate shell can maintain the droplet shape and retains the Matrigel® and collagen components in the droplet core while they undergo the slower gelation process.

Environmental temperature control is crucial for success in fabricating structures from materials such as collagen or Matrigel®. Matrigel® matrix is depolymerized around 4 to 6 °C, starts to gel above 10 °C, and gels rapidly at 22–35 °C.[25,47] Collagen molecules will self-assemble and aggregate to form fibrils under various conditions. Collagen gelation conditions are dependent on temperature, pH, ionic strength, surfactants, the presence of glycerol and sugars, and the non-helical ends of the molecules.[48–50] At room temperature (around 21 °C), collagen viscosity rapidly increases as the pH is increased from 3.5 to 5.5, indicating the onset of gelation.[51] In this work, pH was kept around 7.4 and the temperature was kept low by cooling both the reservoir as well as the flow path through which the solution is delivered to the microfluidic chip. Chilling was achieved using a concentric tube heat exchanger, in which the collagen + Matrigel® + alginate + cell solution was flowed through the tube, and ice-cold water was flowed through the annulus. The beads were generated at a rate of approximately two per second. The beads showed a clear boundary between the core and the shell layers. The MCF-7 cells formed 190 μm diameter compact spheroids after 8 days culture (Fig. 3).

B. MCF-7 cells proliferate inside the core of the core-shell beads

The cells proliferated in the three-dimensional hydrogel environment to form multicellular spheroids. Addition of Matrigel® to the bead core resulted in faster MCF-7 cell proliferation compared to beads which contained only alginate, or to beads which contained only collagen + alginate (Fig. 4). Addition of Matrigel® to the bead core contributed to more uniform spheroid sizes compared to beads which contained either only alginate, or collagen + alginate (Fig. 5).

The Student's two-sided t-test was used to evaluate the statistical significance of the results. The proliferation of cells was significantly different between collagen + alginate beads and Matrigel® + collagen + alginate beads ($P < 0.01$). The proliferation of cells was also significantly different between Matrigel® + collagen + alginate beads and alginate-only beads ($P < 0.05$).

These trends in proliferation rate follow trends observed in the literature: previous work has found that Matrigel®, which includes laminin, collagen IV, entactin, as well as growth factors and other proteins, has been found to promote tumor growth.[25] In contrast, pure collagen I gels do not produce the same cell behavior.[25] Previous work studying MCF-7 cells in collagen

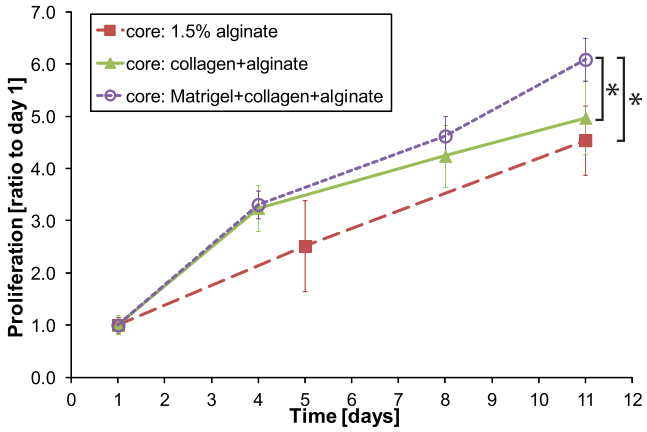

FIG. 4. Comparison of MCF-7 cell proliferation in pure alginate core-shell beads, core (collagen + alginate mixture)-shell beads, and core (Matrigel® + collagen + alginate mixture)-shell beads. Proliferation was measured using a standard MTS assay. Data represent the averages of triplicate determinations; bars represent standard deviation.

has used collagen concentration in the range of 1 mg/ml[26] to 2 mg/ml.[52,53] Our work shows that the use of reconstituted basement matrix in conjunction with collagen is important for proliferation of MCF-7 cells encapsulated within the beads. Although the Matrigel® alone may be sufficient for promoting cell proliferation and spheroid formation[33] in MCF-7 cells,[26] the reconstituted basement membrane is a complex mixture containing growth factors which can also influence cellular behavior in addition to the ECM proteins. Matrigel® contains a mixture of extracellular matrix proteins such as laminin and collagen IV, but also growth factors[25] such as transforming growth factor beta (TGF-β) and insulin-like growth factor 1 (IGF-1),[54] which are signaling molecules that are key regulators of development and cancer progression.[55] Proliferative effects and spheroid formation in pure Matrigel® might thus in part be attributed

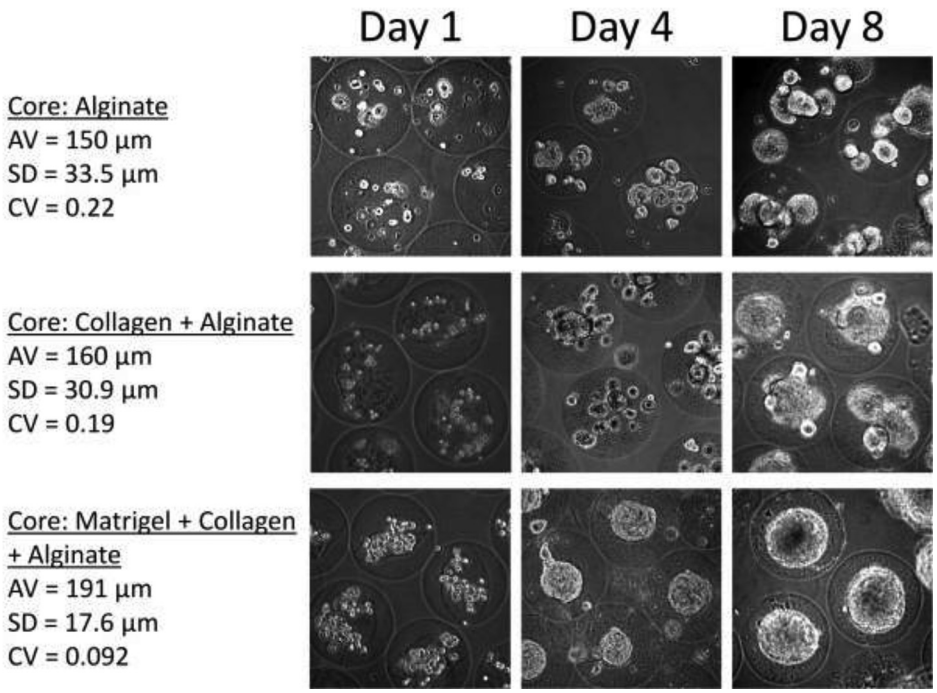

FIG. 5. Size distribution of tumor spheroids. Bead size and spheroid size were measured after 8 days culture. The average diameter (AV), standard deviation (SD), and CV for spheroids are given for each bead type.

the presence of these growth factors. Collagen, nevertheless, remains a major component of the tumor microenvironment. Collagen is the largest structural component in the extracellular matrix, particularly in the environment around tumors.[56–58] Previous work has shown that collagen in the tumor environment is the largest contributor to tissue elastic modulus as well as tissue resistance to drug penetration.[59] The organization of the collagen in the ECM can either promote cell migration when the collagen is in linearized bundles, or impede migration, when the collagen network is dense and cross-linked.[29] Thus, the incorporation of collagen into the hydrogel bead remains an important consideration for a more representative tumor model.

Cell-laden alginate beads have been generated using both emulsion[38,60] as well as microfluidic[31,61] methods. Wang and Wang[33] generated cell-laden core-only beads using Matrigel® + alginate with external gelation (beads gelled off-chip in a $CaCl_2$ bath) with the upper limit of 1:1 alginate:Matrigel® ratio for spherical bead morphology, and when using a long warming tube to help gel the Matrigel®. In that work, the final alginate and Matrigel® droplet diameter was $254 \pm 15.3\ \mu$m. Hong *et al.*[34] generated cell-laden core-only collagen microspheres (3.5 mg/ml collagen) using a microfluidic T-junction, which were gelled on-chip after extraction from the oil phase. That process resulted in spherical beads, with final $272 \pm 12.6\ \mu$m average diameter of the collagen microspheres. In the method presented here, by using internal gelation of the alginate, in addition to a core-shell bead structure, a spherical bead morphology can be readily achieved with final bead uniformity comparable to that from previous work.[33,34]

The alginate shell maintains the cells in three-dimensional culture during the formation of multicellular spheroids. Our previous work[62,63] has found that for some cell lines including MCF-7 cells, a simple core-only bead structure results in out-of-bead cell proliferation, with subsequent cell sedimentation to the bottom of the culture flask and formation of a cell monolayer under the beads over the course of approximately 6 days for the formation of the spheroids. The shell can reduce this monolayer formation during the incubation time, and obviates the need to transfer the beads to a separate culture flask for drug screening. The alginate in the bead core helps to ensure that the beads can be centrifuged and separated from the oil phase after bead generation. Without this alginate in the bead core, the beads are easily broken during the washing steps, resulting in poor cell encapsulation and dispersed cells.

Alternative methods to generate a core-shell structure include a two-step process in which the cores are first formed, followed by a second flow focusing step in which the shell is formed around the core.[62] We have found that collagen + alginate cores can be readily encapsulated inside alginate shells in this way, using an internal gelation process for both the first and second steps.[64] In order to create simple bead cores containing three components (Matrigel® + collagen + alginate) and using internal gelation, calcium carbonate particles should be added to the mixture. However, we found that the addition of Matrigel® to the core mixture caused the calcium carbonate particles to aggregate, resulting in an inhomogeneous mixture. Thus, in the simultaneous core-shell method presented here, the core (Matrigel® + collagen + alginate, no $CaCO_3$) flow is maintained separate from the shell (alginate + $CaCO_3$) flow during the flow focusing process.

C. Second harmonic generation imaging shows collagen distribution within the core-shell beads

Although the beads had a visible boundary between the core and shell layers in bright field microscopy, we used second harmonic generation imaging to characterize, in a label-free manner, the distribution of the collagen which was only added to the solution intended to form the bead core. The non-centrosymmetric molecular assemblies of collagen I fibers allow them to produce bright SHG signals when excited by light in the infrared range.[42,65,66] Overlaid images of the SHG channel with the differential interference contrast images produced by collecting the forward propagated excitation light showed that the collagen was located within the bead cores (Fig. 6). The differential interference contrast images also show a clear boundary between the bead core and shell after bead generation in this one-step microfluidic process.

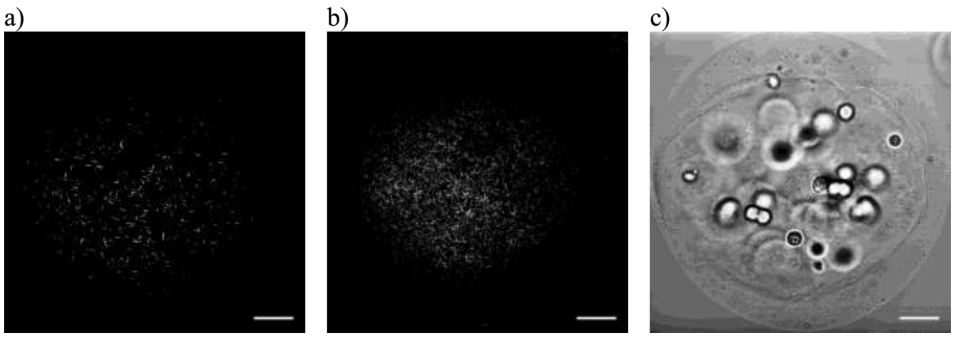

FIG. 6. (a) Back-propagated SHG image of collagen fibers seeded at the core of a one day old MCF-7 core-shell Matrigel® + collagen + alginate bead. The image was acquired at a depth of 150 μm into the 300 μm diameter bead. (b) Maximum intensity z-projection of 31 optical sections acquired at 5 μm intervals from the top of the bead to 300 μm into the specimen. (c) A differential interference contrast image produced by collecting the forward propagated 810 nm excitation light after it passes through the specimen. In this image, the outline of the alginate shell, seeded cells and boundary of the Matrigel® + collagen + alginate core can be identified. Each scale bar represents 100 μm.

D. Drug screening shows multicellular resistance compared to monolayer culture

The three-dimensional, spheroid cultures within the core-shell beads show multicellular resistance compared to 2-D monolayer cultures for tamoxifen (Fig. 7).

The IC_{50} values of both drugs are higher in the 3-D core-shell bead model than in the 2-D monolayer model (Fig. 8). 90% confidence intervals on the nonlinear regression fit parameters including the IC_{50}s were calculated during the fitting process in MATLAB. These indicated that the difference in tamoxifen IC_{50}s between 2-D monolayer and 3-D core-shell bead models was significant while that in the docetaxel IC_{50}s was not. The measured tamoxifen growth inhibition follows trends from literature data, showing inhibition of proliferation in monolayer as well as reduced inhibition when MCF-7 cells are cultured in 3-D.[67–69] The measured docetaxel growth inhibition in these spheroids, which were approximately 200 μm in diameter, was not significantly less than in 2-D monolayer. In the literature, Takagi *et al.*[70] and Breslin and O'Driscoll[17] have found that the degree of multicellular resistance for different drugs can be different, in part due to different mechanisms of action. Docetaxel is incorporated into cytoskeletal microtubules during the G_2/M phases of the cell cycle and thus causes cell death.[71] Jeong *et al.*[72] found that MCF-7 cells acquired higher resistance to docetaxel when their spheroids were almost 700 μm diameter compared to smaller spheroids. These large spheroids had necrotic cores and a peripheral rim of proliferating cells, and they attributed the multicellular resistance to the mechanism of action of the docetaxel.[72] Monazzam *et al.*[73] also found multicellular resistance in MCF-7 cells to docetaxel using spheroids of 1.2 mm diameter.

In contrast, smaller spheroids may have a smaller percentage of quiescent cells, thus leading to less multicellular resistance for docetaxel. Future work can use cells expressing cell cycle

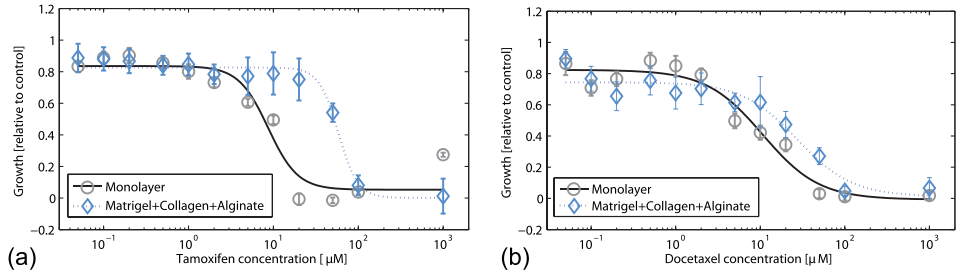

FIG. 7. Effects of tamoxifen and docetaxel on growth inhibition in 2-D monolayer and multicellular spheroids within 3-D core (Matrigel® + collagen + alginate)-shell beads. Monolayer cells were seeded and incubated overnight to permit cell attachment. MCF-7 cells in beads were grown for 8 days to form spheroids before treatment. Then, the cells were exposed to tamoxifen and docetaxel, respectively, for 3 days. The cell growth inhibition was verified by MTS assay. The error bars denote ± SD for N = 3. Growth was as a ratio to untreated culture (control) for each bead type.

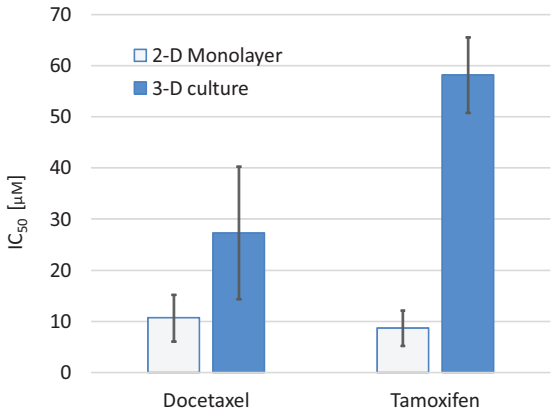

FIG. 8. Antiproliferative effect of anticancer drugs in 2-D monolayer model and 3-D core-shell beads. Docetaxel: IC_{50} was 11 μM in 2-D monolayer, 27 μM in 3-D culture; Tamoxifen: IC_{50} was 9 μM in 2-D monolayer, 58 μM in 3-D culture. 90% confidence intervals on the nonlinear regression fit parameters including the IC_{50}s were calculated during the fitting process.

reporters such as the fluorescence ubiquitination-based cell cycle indicator,[74] which permits visualization of the dynamics of cell cycle progression in live cells through the use of two-color indicators, to help identify the spatial distribution and ratio of proliferating cells to quiescent cells. Using these cell cycle reporters during the drug screening, we could further study and better understand the multicellular resistance for different anticancer drugs in this spheroid culture model.

Although high alginate concentrations in the range of 5% or higher have been used as a barrier to exclude antibody-sized molecules[60] from entering inside alginate capsules, the alginate shells used in the core-shell beads presented here are not expected to hinder the diffusion of drugs such as tamoxifen and docetaxel. Li *et al.*[75] found that the average pore diameter in 1.5% alginate was approximately 147 Å and in 3% alginate was approximately 170 Å. These alginate gels did not present a significant diffusion barrier for vitamin B12 (molecular weight 1300 Da; Stokes radius of $\sim$7.7 Å) compared to diffusion in water. Simpliciano *et al.*[76] found that 1.5% medium viscosity alginate had a median pore size of 5.2 nm. They noted that diffusion was not hindered through this gel for a 4 kDa marker. Smidsrød and Skjåk-Bræk[77] found that the pore diameters in 2% alginate range from 5 to 200 nm. Based on the work of Briššová *et al.*,[78] who studied the permeability and exclusion limits of alginate microcapsules, a 5 nm viscous radius would correspond to a globular protein such as γ-globulin with molecular weight of 158 kDa, while a 200 nm viscous radius would be larger than a globular protein of $>$1000 kDa. Van Elk *et al.*[79] used 3% Manucol LKX alginate, a higher concentration of the same alginate used in the work presented here, and found that fluorescein (0.7 nm, 332.31 g/mol) was able to diffuse freely through their 3% alginate matrix. Based on these previous findings, it is likely that tamoxifen (molecular mass 371.5 g/mol) and docetaxel (molecular mass 807.9 g/mol) are also able to diffuse freely through the alginate shell of the hydrogel beads.

In future work, these core-shell beads could be used to study the influence of pressure on growing tumors by increasing the concentration, and thus the stiffness, of the alginate shell.[32] These core-shell beads could also incorporate tumor-associated fibroblasts or other cells as a co-culture, to study the effects of tumor cell-stromal interactions and other effects on drug response.

IV. CONCLUSIONS

This microfluidic system produces a core-shell structure in which the shell is composed of alginate, and the core is composed of collagen and/or Matrigel® in which cells are dispersed. The core-shell structure allows embedded MCF-7 cells to proliferate and form multicellular

spheroids. The alginate shell serves two functions: (1) it is a fast-gelling hydrogel which helps prevent droplet coalescence and helps maintain droplet sphericity during the slower gelation process of the collagen and Matrigel; (2) it discourages cell proliferation out of the bead, and subsequent formation of a cell monolayer underneath the beads during cell culture. In the core, the addition of extracellular matrix components including both collagen I and reconstituted basement membrane permitted the formation of more uniformly sized MCF-7 cell spheroids compared to spheroids grown in pure alginate beads or those containing collagen I alone. The multicellular spheroids showed drug resistance compared to monolayer for tamoxifen, while the docetaxel growth inhibition in the spheroids was not significantly less than in monolayer.

This core-shell bead generation method enables the production of tumor spheroids surrounded by elements of the extracellular matrix, providing a model of the tumor microenvironment with applications for drug screening assays. Future work will examine the re-organization and remodelling of the collagen around cells of different collagen contractility.

ACKNOWLEDGMENTS

Part of this work was carried out in the AMPEL Nanofabrication Facility. This work was funded by the Natural Science and Engineering Research Council of Canada and the Canadian Institutes of Health Research, and supported by a Canadian Breast Cancer Foundation doctoral fellowship awarded to S.M.G. Imaging was conducted at the UBC BioImaging Facility. Dr. Marcel Bally at the BC Cancer Research Centre kindly provided the MCF-7 cells as well as clinical formulations of docetaxel and tamoxifen.

[1]D. C. Swinney and J. Anthony, Nat. Rev. Drug Discovery **10**(7), 507–519 (2011).
[2]Z. E. Perlman, M. D. Slack, Y. Feng, T. J. Mitchison, L. F. Wu, and S. J. Altschuler, Science **306**(5699), 1194–1198 (2004).
[3]M. G. Rubashkin, G. Ou, and V. M. Weaver, Biochemistry **53**(13), 2078–2090 (2014).
[4]J. Comley, Drug Discovery World Fall **2010**, 25–41.
[5]K. J. Martin, D. R. Patrick, M. J. Bissell, and M. V. Fournier, PLoS ONE **3**(8), e2994 (2008).
[6]C. M. Nelson and M. J. Bissell, Annu. Rev. Cell Dev. Biol. **22**(1), 287–309 (2006).
[7]A. Abbott, Nature **424**(6951), 870–872 (2003).
[8]M. J. Bissell and D. Radisky, Nat. Rev. Cancer **1**(1), 46–54 (2001).
[9]R. Sutherland, Science **240**(4849), 177–184 (1988).
[10]R. M. Sutherland, B. Sordat, J. Bamat, H. Gabbert, B. Bourrat, and W. Mueller-Klieser, Cancer Res. **46**(10), 5320–5329 (1986); PubMed ID (PMID): 3756881.
[11]A. I. Minchinton and I. F. Tannock, Nat. Rev. Cancer **6**(8), 583–592 (2006).
[12]R.-Z. Lin and H.-Y. Chang, Biotechnol. J. **3**(9-10), 1172–1184 (2008).
[13]D. V. LaBarbera, B. G. Reid, and B. H. Yoo, Expert Opin. Drug Discovery **7**(9), 819–830 (2012).
[14]G. Hamilton, Cancer Lett. **131**(1), 29–34 (1998).
[15]A. Ivascu and M. Kubbies, Int. J. Oncol. **31**(6), 1403–1413 (2007).
[16]A. Asthana and W. S. Kisaalita, Drug Discovery Today **17**(15–16), 810–817 (2012).
[17]S. Breslin and L. O'Driscoll, Drug Discovery Today **18**(5–6), 240–249 (2013).
[18]A. Nagy Mehesz, J. Brown, Z. Hajdu, W. Beaver, J. V. L. d. Silva, R. P. Visconti, R. R. Markwald, and V. Mironov, Biofabrication **3**(2), 025002 (2011).
[19]A. Hsiao, Y.-C. Tung, C.-H. Kuo, B. Mosadegh, R. Bedenis, K. Pienta, and S. Takayama, Biomed. Microdev. **14**(2), 313–323 (2012).
[20]A. Y. Hsiao, Y.-C. Tung, X. Qu, L. R. Patel, K. J. Pienta, and S. Takayama, Biotechnol. Bioeng. **109**(5), 1293–1304 (2012).
[21]J. M. Kelm, N. E. Timmins, C. J. Brown, M. Fussenegger, and L. K. Nielsen, Biotechnol. Bioeng. **83**(2), 173–180 (2003).
[22]C. D. Roskelley and M. J. Bissell, Semin. Cancer Biol. **12**(2), 97–104 (2002).
[23]C. D. Roskelley, A. Srebrow, and M. J. Bissell, Curr. Opin. Cell Biol. **7**(5), 736–747 (1995).
[24]M. R. Dusseiller, M. L. Smith, V. Vogel, and M. Textor, Biointerphases **1**(1), P1–P4 (2006).
[25]R. Fridman, G. Benton, I. Aranoutova, H. K. Kleinman, and R. D. Bonfil, Nat. Protoc. **7**(6), 1138–1144 (2012).
[26]S. Krause, M. V. Maffini, A. M. Soto, and C. Sonnenschein, BMC Cancer **10**, 263 (2010).
[27]P. P. Provenzano, D. R. Inman, K. W. Eliceiri, S. M. Trier, and P. J. Keely, Biophys. J. **95**(11), 5374–5384 (2008).
[28]J. A. Joyce and J. W. Pollard, Nat. Rev. Cancer **9**(4), 239–252 (2009).
[29]P. Lu, V. M. Weaver, and Z. Werb, J. Cell Biol. **196**(4), 395–406 (2012).
[30]L. Yu, M. C. W. Chen, and K. C. Cheung, Lab Chip **10**(18), 2424–2432 (2010).
[31]V. L. Workman, S. B. Dunnett, P. Kille, and D. D. Palmer, Biomicrofluidics **1**(1), 014105–014109 (2007).
[32]K. Alessandri, B. R. Sarangi, V. V. Gurchenkov, B. Sinha, T. R. Kießling, L. Fetler, F. Rico, S. Scheuring, C. Lamaze, A. Simon, S. Geraldo, D. Vignjević, H. Doméjean, L. Rolland, A. Funfak, J. Bibette, N. Bremond, and P. Nassoy, Proc. Natl. Acad. Sci. USA **110**(37), 14843–14848 (2013).
[33]Y. Wang and J. Wang, Analyst **139**(10), 2449–2458 (2014).
[34]S. Hong, H.-J. Hsu, R. Kaunas, and J. Kameoka, Lab Chip **12**(18), 3277–3280 (2012).

[35]G. M. Whitesides, E. Ostuni, S. Takayama, X. Jiang, and D. E. Ingber, Annu. Rev. Biomed. Eng. **3**, 335–373 (2001).
[36]H. J. Phillips, in *Tissue Culture: Methods and Applications*, edited by P. F. Kruse and M. K. Patterson (Academic Press, 1973), pp. 406–408.
[37]S. L. Anna, N. Bontoux, and H. A. Stone, Appl. Phys. Lett. **82**(3), 364–366 (2003).
[38]D. Poncelet, R. Lencki, C. Beaulieu, J. P. Halle, R. J. Neufeld, and A. Fournier, Appl. Microbiol. Biotechnol. **38**(1), 39–45 (1992).
[39]H. Zhang, E. Tumarkin, R. M. A. Sullan, G. C. Walker, and E. Kumacheva, Macromol. Rapid Commun. **28**(5), 527–538 (2007).
[40]L. Huyck, C. Ampe, and M. V. Troys, Assay Drug Dev. Technol. **10**(4), 382–392 (2012).
[41]W. Y. Ho, S. K. Yeap, C. L. Ho, R. A. Rahim, and N. B. Alitheen, PLoS ONE **7**(9), e44640 (2012).
[42]W. R. Zipfel, R. M. Williams, R. Christie, A. Y. Nikitin, B. T. Hyman, and W. W. Webb, Proc. Natl. Acad. Sci. USA **100**(12), 7075–7080 (2003).
[43]E. Coezy, J. Borgna, and H. Rochefort, Cancer Res. **42**(1), 317–323 (1982); PubMed ID (PMID): 7053859.
[44]M. Qadir, B. Kwok, W. Dragowska, K. To, D. Le, M. Bally, and S. Gorski, Breast Cancer Res. Treat. **112**(3), 389–403 (2008).
[45]D. L. Morse, H. Gray, C. M. Payne, and R. J. Gillies, Mol. Cancer Ther. **4**(10), 1495–1504 (2005).
[46]K. Pataky, T. Braschler, A. Negro, P. Renaud, M. P. Lutolf, and J. Brugger, Adv. Mater. **24**(3), 391–396 (2012).
[47]See http://csmedia2.corning.com/LifeSciences/Media/pdf/faq_DL_026_Corning_Matrigel_Matrix.pdf for Corning® Matrigel® Matrix Frequently Asked Questions, CLS-DL-CC-026 (2013).
[48]S. Leikin, D. C. Rau, and V. A. Parsegian, Nat. Struct. Mol. Biol. **2**(3), 205–210 (1995).
[49]Y. Li, A. Asadi, M. R. Monroe, and E. P. Douglas, Mater. Sci. Eng.: C **29**(5), 1643–1649 (2009).
[50]M. Achilli and D. Mantovani, Polymers **2**(4), 664–680 (2010).
[51]E. A. Roth, T. Xu, M. Das, C. Gregory, J. J. Hickman, and T. Boland, Biomaterials **25**(17), 3707–3715 (2004).
[52]C.-L. Chiu, M. A. Digman, and E. Gratton, J. Biophys. **2013**, 8.
[53]Q. Shi, R. P. Ghosh, H. Engelke, C. H. Rycroft, L. Cassereau, J. A. Sethian, V. M. Weaver, and J. T. Liphardt, Proc. Natl. Acad. Sci. USA **111**(2), 658–663 (2014).
[54]S. Vukicevic, H. K. Kleinman, F. P. Luyten, A. B. Roberts, N. S. Roche, and A. H. Reddi, Exp. Cell Res. **202**(1), 1–8 (1992).
[55]L. Walsh and S. Damjanovski, Cell Commun. Signaling **9**(1), 10 (2011).
[56]C. S. Szot, C. F. Buchanan, J. W. Freeman, and M. N. Rylander, Biomaterials **32**(31), 7905–7912 (2011).
[57]S. M. Kakkad, M. Solaiyappan, P. Argani, S. Sukumar, L. K. Jacobs, D. Leibfritz, Z. M. Bhujwalla, and K. Glunde, J. Biomed. Opt. **17**(11), 116017 (2012).
[58]S. Ramanujan, A. Pluen, T. D. McKee, E. B. Brown, Y. Boucher, and R. K. Jain, Biophys. J. **83**(3), 1650–1660 (2002).
[59]P. A. Netti, D. A. Berk, M. A. Swartz, A. J. Grodzinsky, and R. K. Jain, Cancer Res. **60**(9), 2497–2503 (2000); PubMed ID (PMID): 10811131.
[60]C. A. Hoesli, R. L. J. Kiang, D. Mocinecová, M. Speck, D. J. Mošková, C. Donald-Hague, I. Lacík, T. J. Kieffer, and J. M. Piret, J. Biomed. Mater. Res. B **100B**(4), 1017–1028 (2012).
[61]V. L. Workman, S. B. Dunnett, P. Kille, and D. D. Palmer, Macromol. Rapid Commun. **29**(2), 165–170 (2008).
[62]L. Yu, C. Ni, S. M. Grist, C. Bayly, and K. C. Cheung, Biomed. Microdev. **17**(2), 33 (2015).
[63]C. Bayly, L. Yu, and K. C. Cheung, in *The 17th International Conference on Miniaturized Systems for Chemistry and Life Sciences, MicroTAS 2013* (Freiburg, Germany, 2013), pp. 1710–1712.
[64]C. Bayly, L. Yu, and K. C. Cheung, in Biomedical Engineering Society Annual Meeting (BMES 2013) (Seattle, USA, 2013).
[65]G. Cox, E. Kable, A. Jones, I. Fraser, F. Manconi, and M. D. Gorrell, J. Struct. Biol. **141**(1), 53–62 (2003).
[66]G. Cox and E. Kable, in *Cell Imaging Techniques*, edited by D. Taatjes and B. Mossman (Humana Press, 2006), Vol. 319, pp. 15–35.
[67]T. Rossi, V. Iannuccelli, G. Coppi, E. Bruni, and G. Baggio, Anticancer Res. **29**(11), 4529–4533 (2009); PubMed ID (PMID): 20032401.
[68]H. K. Dhiman, A. R. Ray, and A. K. Panda, Biomaterials **26**(9), 979–986 (2005).
[69]J. L. Horning, S. K. Sahoo, S. Vijayaraghavalu, S. Dimitrijevic, J. K. Vasir, T. K. Jain, A. K. Panda, and V. Labhasetwar, Mol. Pharmaceutics **5**(5), 849–862 (2008).
[70]A. Takagi, M. Watanabe, Y. Ishii, J. Morita, Y. Hirokawa, T. Matsuzaki, and T. Shiraishi, Anticancer Res. **27**(1A), 45–53 (2007); PubMed ID (PMID): 17352215.
[71]E. S. Antonarakis and A. J. Armstrong, Prostate Cancer Prostatic Dis. **14**(3), 192–205 (2011).
[72]E. K. Jeong, S. Y. Lee, H. M. Jeon, M. K. Ju, C. H. Kim, and H. S. Kang, Int. J. Oncol. **37**(3), 655–661 (2010).
[73]A. Monazzam, R. Josephsson, C. Blomqvist, J. Carlsson, B. Langstrom, and M. Bergstrom, Breast Cancer Res. **9**(4), R45 (2007).
[74]A. Sakaue-Sawano, H. Kurokawa, T. Morimura, A. Hanyu, H. Hama, H. Osawa, S. Kashiwagi, K. Fukami, T. Miyata, H. Miyoshi, T. Imamura, M. Ogawa, H. Masai, and A. Miyawaki, Cell **132**(3), 487–498 (2008).
[75]R. H. Li, D. H. Altreuter, and F. T. Gentile, Biotechnol. Bioeng. **50**(4), 365–373 (1996).
[76]C. Simpliciano, L. Clark, B. Asi, N. Chu, M. Mercado, S. Diaz, M. Goedert, and M. Mobed-Miremadi, J. Surf. Eng. Mater. Adv. Technol. **3**(4A), 1–12 (2013).
[77]O. Smidsrød and G. Skjåk-Braek, Trends Biotechnol. **8**(0), 71–78 (1990).
[78]M. Briššová, M. Petro, I. Lacík, A. C. Powers, and T. Wang, Anal. Biochem. **242**(1), 104–111 (1996).
[79]M. van Elk, C. Lorenzato, B. Ozbakir, C. Oerlemans, G. Storm, F. Nijsen, R. Deckers, T. Vermonden, and W. E. Hennink, "Alginate microgels loaded with temperature sensitive liposomes for magnetic resonance imageable drug release and microgel visualization," Eur. Polym. J. (published online 2015).